Published in final edited form as:
Future Microbiol. 2013 February ; 8(2): 257–269. doi:10.2217/fmb.12.134.

Peptide targeting and imaging of damaged lung tissue in influenza-infected mice

Na Li[1,2], **Lu Yin**[1], **Damien Thévenin**[3], **Yoshiyuki Yamada**[1], **Gino Limmon**[1], **Jianzhu Chen**[4], **Vincent TK Chow**[2], **Donald M Engelman**[3], and **Bevin P Engelward**[*,5]

[1]Interdisciplinary Research Group in Infectious Diseases, Singapore–Massachusetts Institute of Technology Alliance in Research & Technology, 1 CREATE Way, #03–12/13/14 Enterprise Wing, 138602, Singapore

[2]Department of Microbiology, National University of Singapore, 5 Science Drive 2, Block MD4 Level 3, 117597, Singapore

[3]Department of Molecular Biophysics & Biochemistry, Yale University, 266 Whitney Avenue, PO Box 208114, New Haven, CT 06520-8114, USA

[4]The David H Koch Institute for Integrative Cancer Research at MIT, 500 Main Street, MIT building 76-243, Cambridge, MA 02142, USA

[5]Department of Biological Engineering, Massachusetts Institute of Technology, Building 56, Room 631, 77 Massachusetts Avenue, Cambridge, MA 02139, USA

Abstract

Aim—In this study, we investigate whether pH (low) insertion peptide (pHLIP) can target regions of lung injury associated with influenza infection.

Materials & methods—Fluorophore-conjugated pHLIP was injected intraperitoneally into mice infected with a sublethal dose of H1N1 influenza and visualized histologically.

Results—pHLIP specifically targeted inflamed lung tissues of infected mice in the later stages of disease and at sites where alveolar type I and type II cells were depleted. Regions of pHLIP-targeted lung tissue were devoid of peroxiredoxin 6, the lung-abundant antioxidant enzyme, and were deficient in pneumocytes. Interestingly, a pHLIP variant possessing mutations that render it insensitive to pH changes was also able to target damaged lung tissue.

[*]Author for correspondence: bevin@mit.edu.

Author contributions Conceived and designed the experiments: N Li and BP Engelward. Performed the experiments: N Li. Analyzed the data: N Li and L Yin. Design of quantification algorithms: L Yin. Peptide–fluorophore conjugate synthesis: D Thévenin. Contributed materials/analysis tools: Y Yamada, G Limmon, J Chen, VTK Chow, DM Engelman and BP Engelward. Wrote the paper: N Li and BP Engelward.

Disclaimer The views expressed herein are solely the responsibility of the authors and do not necessarily represent the official views of the Singapore National Research Foundation.

Financial & competing interests disclosure The authors have no other relevant affiliations or financial involvement with any organization or entity with a financial interest in or financial conflict with the subject matter or materials discussed in the manuscript apart from those disclosed.

Ethical conduct of research The authors state that they have obtained appropriate insti tutional review board approval or have followed the principles outlined in the Declaration of Helsinki for all human or animal experimental investigations. In addition, for investi gations involving human subjects, informed consent has been obtained from the participants involved.

Conclusion—pHLIP holds potential for delivering therapeutics for lung injury during influenza infection. Furthermore, there may be more than one mechanism that enables pHLIP variants to target inflamed lung tissue.

Keywords

delivery; inflammation; influenza; peptide; pHLIP

Many influenza-related deaths are not directly linked to virus infection, but instead can be attributed to an exaggerated or dysregulated immune response towards the pathogenic insult [1,2]. Hence, effective delivery of therapeutic agents aimed at ameliorating lung injury that is exacerbated by inflammation could greatly improve the survival and recovery of patients severely infected with influenza.

In this study, we set out to develop a strategy for targeting inflamed or injured regions of the lungs in order to enable delivery of pharmaceutical agents. It was previously reported that an approximately 36-amino acid pH-responsive peptide is able to target inflamed arthritic joints in mice [3]. This peptide, named pH (low) insertion peptide (pHLIP), has a strong affinity for low-pH microenvironments such as tumors [4–6], where it inserts into the cell membrane with a change in conformation and the release of approximately 2 kcal/mole of energy. The energy released supports translocation of cargos conjugated to its C-terminus into the cytoplasm, making pHLIP a nanosyringe for small, cell-impermeable molecules such as phalloidin and peptide nucleic acid [7–9]. While most healthy organs are usually slightly alkaline (~pH 7.2–7.4) under physiological conditions, the interstitium of inflamed tissue has a much lower pH (as low as pH 5.8) [10,11]. Thus, influenza-induced lung inflammation may facilitate specific targeting of pHLIP. While extensive studies have been performed to evaluate pHLIP and to test its efficacy in the context of cancer, nothing had been done to test its utility as a means for targeting inflamed tissue associated with infection. Here, we have evaluated the ability of pHLIP to specifically target inflamed regions of the lung following infection with influenza.

To study pHLIP targeting of inflammation and associated lung injury, we examined the biodistribution of pHLIP in a C57Bl/6 murine model inoculated with an H1N1 variant of influenza, influenza A/Puerto Rico/8/34 (PR8). A high sublethal dose of PR8 infection in C57Bl/6 mice causes severe viral pneumonia, which is a principal characteristic of hospitalized or intensive care pandemic H1N1 patients [12–14]. Knowledge regarding the specific biodistribution of pHLIP is critical for evaluating its potential utility both as a bioimaging tool and as a delivery agent for therapeutic drugs. This study shows that pHLIP specifically targets inflamed lung tissue, and does not accumulate in noninflamed lung tissue. pHLIP-targeted regions are devoid of healthy pneumocytes, indicating that pHLIP specifically targets damaged regions of the lung. Importantly, these regions are also deficient in peroxiredoxin 6, an important lung-abundant antioxidant produced by alveolar type I (ATI) cells in response to inflammation. These findings bring about new possibilities for detecting inflammation-induced lung damage and for specific delivery of therapeutic agents, such as antioxidants, to regions of lung injury.

Interestingly, a peptide, known as K-pHLIP, which is similar to pHLIP but without the ability to behave in a pH-responsive fashion, was also able to target damaged lung tissue, suggesting the possibility of more than one mechanism by which pHLIP targeted damaged lung tissue during influenza. Together, these results suggest there is more than one mechanism for the targeted delivery of pHLIP-conjugated agents to sites of pulmonary inflammation and lung injury.

Materials & methods

Peptide synthesis & conjugation with fluorescent dye

The pHLIP peptide variant used in this study was synthesized with a cysteine residue at its N-terminus by solid-phase peptide synthesis and purified by reverse-phase high-performance liquid chromatography at the WM Keck Foundation Biotechnology Resource Laboratory (Yale University, CT, USA). It has the following sequence: AC̲EQNPIYWARYADWLFTTPLLLLDLALLVDADEGTG. Fluorescent dyes were conjugated to the N-terminal cysteine of pHLIP using the following protocol: to a solution of pHLIP peptide (1 μmol) in a solvent mixture consisting of 1:1:3:5 of dimethylformamide, dimethyl sulfoxide, methanol, and aqueous NH_4HCO_3 buffer (200 mM; pH 8) was added 1 eq. of Alexa Fluor® 647 C2 maleimide (Invitrogen, CA, USA) in 50 μl dimethyl sulfoxide. This mixture was stirred at room temperature and in the dark for 10 min. To this reduced mixture, an oxidizing solution of $K_3Fe(III)CN_6$ (6 mg, 18.2 μmol, 23.1 eq.) in 60 μl of aqueous NH_4HCO_3 buffer (200 mM; pH 8) was added. This reaction mixture was stirred at room temperature for 3 h. The desired product was isolated via reverse-phaseg HPLC (Hewlett Packard Zorbax® semiprep 9.4 × 250 mm SB-C18 column; flow rate: 2 ml/min; phase A: water + 0.01% trifluoroacetic acid; phase B: acetonitrile + 0.01% trifluoroacetic acid; gradient: 70 min from 99:1 A/B to 1:99 A/B). In subsequent experiments, Hylite Fluor® 647-conjugated pHLIP and K-pHLIP (AC̲EQNPIYWARYAKWLFTTPLLLL**K**LALLVDADEGTG) was purchased from AnaSpec (CA, USA). The purity was ≥90%, as confirmed by analytical HPLC.

Animal studies

This study was carried out in strict accordance with the National Advisory Committee for Laboratory Animal Research (NACLAR) guidelines (Guidelines on the Care and Use of Animals for Scientific Purposes) in facilities licensed by the Agri-Food and Veterinary Authority of Singapore (AVA), the regulatory body of the Singapore Animals and Birds Act. The protocol was approved by the Institutional Animal Care and Use Committee (IACUC), National University of Singapore (permit number: IACUC 117/10).

Viral infection

Eight- to twelve-week-old female inbred C57Bl/6 mice were purchased from the Biological Resource Centre (BRC) and Comparative Medicine/Centre for Animal Resources of National University of Singapore (CARENUS). All mice were housed in the animal vivarium at the National University of Singapore (NUS). H1N1 PR8 was propagated in chick embryos and titered with plaque assay. Mice were anesthetized with 75 mg/kg of ketamine and 1 mg/kg of medatomidine was instilled intratracheally with 30 PFU/75 μl/mouse of PR8. They were then revived with 1 mg/kg of antipamezole. Mice were monitored for 12 days for weight loss and disease symptoms.

Plaque assay of lung homogenates

Three uninfected or PR8-infected mice were sacrificed on days 5, 7 and 9 postinfection. The cardiac lobes of mice lungs were frozen and homogenized in 400 μl of phosphate-buffered saline (PBS) with gentleMACS™ (Miltenyi Biotec, Germany) and centrifuged at 10,000 rpm for 10 min at 4°C. Cell-free lung homogenate was used in the plaque assay. The PFU values were normalized against total protein (according to the Bradford assay).

Peptide administration & tissue collection

Mice were injected intraperitoneally with 100 μM (in 100 μl) of fluorescently labeled pHLIP or K-pHLIP on days 1, 5 and 10 postinfection. Two days after peptide injection, the

mice were euthanized. Lungs, heart, spleen, liver and kidneys were harvested and fixed in 10% neutral-buffered formalin overnight at 4°C. Fixed tissues were then dehydrated in sequentially higher concentrations of ethanol and embedded in paraffin.

Histology & immunofluorescence

Transverse sections (5 μm) were dewaxed and rehydrated. Antigen retrieval was performed using proteinase K (20 μg/ml in TE buffer, pH 8.0) and hot citric acid buffer treatment (10 mM citric acid, pH 6.0) as needed, depending upon the antibodies. Primary antibodies included anti-fibronectin (Sigma Aldrich, MO, USA), anti-podoplanin (anti-Pdpn; R&D systems), anti-CCSP (Santa Cruz, CA, USA), anti-Prdx6 (Abcam, UK) and anti-surfactant protein C (SPC; Santa Cruz). Antibodies were incubated overnight at 4°C. Tissue sections were stained with Alexa Fluor 488- or Alexa Fluor® 546-conjugated secondary antibodies (Molecular Probes, Invitrogen) for 1 h at room temperature, washed and mounted with ProLong® Gold Antifade with DAPI (Invitrogen). Fluorescence images were taken with a Carl Zeiss scanning microscope, before counter-staining the tissue samples with hematoxylin and eosin (H&E).

For wheat germ agglutinin (WGA) staining, tissue sections were dewaxed and rehydrated according to the usual procedure. After 10 min, at 100°C in hot citric acid buffer, sections are stained for 1 h at room temperature with WGA–Alexa Fluor 488 (20 μg/ml, Molecular Probes; gift from T Tan, Singapore–MIT Alliance for Research and Technology, Singapore).

In vitro assay

Chamber slides were prepared with A549 cells (~5×10^4), cultured for 24 h and rinsed twice with PBS adjusted to pH 5, 6, 7.4 and 8. Following incubation with 8 μM of 5-carboxyfluorescein-conjugated pHLIP in PBS with appropriate pH (30 min, room temperature, in the dark), cells were washed with the appropriate pH-adjusted PBS and viewed under a fluorescence microscope. Cells were washed with the appropriate pH-adjusted PBS and viewed under a fluorescence microscope.

Feature extraction & pHLIP quantification

Infiltrated regions were identified by setting a threshold to segment darker-stained regions of infiltrated regions from uninfiltrated regions based on images of H&E-stained whole-lung sections (n = 3, two sections per mouse). Within the infiltrated region, a smaller threshold was then applied to demarcate heavily and moderately infiltrated regions. Masks of heavily infiltrated, moderately infiltrated and uninfiltrated regions were generated. Details of the quantification algorithm are described in ‘Imaging-based quantification of infiltration’ section.

Moderately infiltrated regions were confirmed at 20–40× magnification by thickening of alveolar walls and the presence of infiltration in the alveolar spaces that involves less than 70% of the total lung parenchyma. These regions were visibly distinguishable from heavily infiltrated sites, which were defined as densely stained regions with infiltration occupying more than 70% of the lung parenchyma.

The extent of colocalization of Alexa Fluor 647-conjugated pHLIP with uninfiltrated, moderately and heavily infiltrated regions was assessed. Total pHLIP was identified by thresholding the intensity of each pixel in Alexa Fluor 647-conjugated pHLIP-containing images. The percentage of pHLIP in heavily infiltrated regions, moderately infiltrated regions and uninfiltrated regions was calculated by the ratio of pHLIP within each mask to total pHLIP, respectively.

ATI cells were identified by thresholding the intensity of each pixel in tissue sections stained with anti-Pdpn. Holes among ATI cells, representing the alveolar spaces, were filled to form the mask of healthy areas; damaged areas were segmented by subtracting healthy areas from total lung sections. The percentage of pHLIP-positive pixels within healthy and damaged regions was computed. Two whole-lung sections from each mouse (n = 3 for uninfected and PR8-infected groups) were used for calculation. Similarly, Prdx6-positive regions were identified by thresholding Prdx6 intensity. The percentage of total pHLIP-induced pixels was calculated in Prdx6-positive regions and Prdx6-negative regions. All image processing and computation algorithms were performed with Matlab (The Math Works, Inc., MA, USA). The codes for the algorithms are available on request.

Imaging-based quantification of infiltration

Ten 5-μm thick transverse lung sections 50 μm apart from each other were obtained from infected mice given or not given Hylite Fluor 647 pHLIP. The sections were then stained with H&E and quantified for the percentage of lung tissue with severe infiltration or consolidation. Original RGB images of H&E-stained tissue sections were converted to grayscale. One intensity threshold was set to exclude large empty spaces, including bronchi, trachea and large blood vessels, from the total section area to obtain the alveolar region. Another intensity threshold was set to segment regions of infiltrated lung parenchyma that were darkly stained with H&E from uninfiltrated regions that possess lightly stained lung parenchyma. The percentage was computed from regions of infiltration and the total alveolar region. The Matlab algorithm used for this purpose is now reported in a manuscript under review [Yin L, Xu S, Chen J *et al*. Quantification of cell dynamics in the lung following influenza virus infection (2013), Submitted].

Statistical analysis

Each result is expressed as mean ± standard error of mean unless otherwise stated. Statistical analyses were performed by analysis of variance or Student's *t*-test. A value of $p < 0.05$ was considered to be statistically significant.

Results

Infection & inflammation kinetics in PR8-infected mice

Using an established influenza mouse model, here we explore the potential utility of pHLIP as a tool for controlling spatiotemporal delivery of therapeutic or imaging agents. C57Bl/6 mice were infected with a sublethal dose of H1N1 PR8. The infection kinetics of this model have been previously reported by our group and Kumar *et al.* These studies show that PR8-infected C57Bl/6 mice experience weight loss from day 4 postinfection, and continue to lose weight until they reached minimum weights at approximately days 10–11 postinfection. This was also the time when maximal lung damage was observed. Thereafter, all mice survived and gradually regained preinfection lung histology at day 21 postinfection [15,16].

In this model, viral titer rises quickly during the first few days, peaking at day 5 postinfection (6.2×10^4 PFU/mg of protein); thereafter, the virus is rapidly reduced on day 7 postinfection (1.3×10^4 PFU/mg of protein), with very little evidence of viral particles by day 9 postinfection (Figure 1A). Importantly, inflammation persists even after viral clearance. Inflammation in the lung tissue is observed histologically via the presence of cellular infiltration that can be readily identified by high nuclear density of immune cells. There is a gradual increase in the amount of cellular infiltration into the lung parenchyma, which leads to condensed alveolar spaces towards the later stages of influenza infection. Consolidation of the alveoli is observed at approximately day 11 postinfection, in which the alveolar spaces are densely packed with fluid and immune cells, as can be observed in H&E

sections (Figure 1B). Since infection and inflammation are causes of tissue acidification, we hypothesized that pHLIP could potentially target inflamed lung tissue.

pHLIP targets influenza-infected lungs

To test for pHLIP targeting to lung tissue affected by influenza-induced pneumonia, we conjugated Alexa Fluor 647 and Hylite Fluor 647 to pHLIP on its noninserting N-terminus to enable visualization of pHLIP in fresh or fixed tissue. Labeled pHLIP was administered on day 10 postinfection and organs were harvested 2 days later to allow time for pHLIP to target the inflamed tissue and to clear from other tissues. No significant auto-fluorescence was observed in mice that did not receive pHLIP (Figure 2A & 2C), and there was no significant accumulation of pHLIP in the lungs of healthy mice (Figure 2B). On the other hand, we observed significant pHLIP-associated fluorescence in the lungs of infected mice (Figure 2D). Unconjugated Alexa Fluor 647 dye was also administered to mice (n = 2) in the same molarity and no significant fluorescence was detected in tissue sections of these mice (data not shown).

pHLIP colocalizes with regions of infiltration

Analysis of H&E-stained lung tissue reveals that the severity of inflammation is highly variable throughout the lungs (intensity of nuclear staining [dark blue/purple] indicates the density of immune cell infiltration), wherein the most densely infiltrated regions are considered to be consolidated (Figure 2G & 2H). Hence, we proceeded to determine the extent to which the degree of cellular infiltration impacts pHLIP targeting. A comparison of the H&E-stained tissue and the localization of pHLIP (compare Figure 2D & 2H) shows that pHLIP colocalizes specifically to the densely infiltrated regions of the lung.

To quantify the association of pHLIP within regions of low and high infiltration, the degree of alveolar infiltration and the percentage of pHLIP-induced fluorescence in the total lung area were assessed. Using an in-house automated quantification program, we demarcated regions based upon the extent of infiltration by thresholding H&E images of whole-lung sections. The method is demonstrated in Figure 3A. Figure 3A has four columns in which the left-most column is an image of the original H&E-stained lung section. The quantification program first identified heavily and moderately infiltrated regions, which are traced out by blue lines shown in the second column. In each region, alveoli, bronchi and blood vessels were filled to generate an alveolar area (third column). Total pHLIP-induced fluorescence that overlapped with heavily and moderately infiltrated regions (right-most column) was then quantified. The total pHLIP-induced fluorescence found in these regions was quantified (right-most images). We calculated that only approximately 1% of pHLIP was in uninfiltrated regions, approximately 13% of pHLIP was in moderately infiltrated regions and approximately 85% of pHLIP was in heavily infiltrated regions (Figure 3B). This further confirms that pHLIP preferentially targets regions of infiltration. To find out whether pHLIP administration elevates infiltration, we quantified the amount of infiltration in the lungs of infected mice compared with infected mice injected with pHLIP. Results show that pHLIP does not increase the amount of lung infiltration in infected mouse lungs (Figure 3C). The data are consistent with our hypothesis that pHLIP targets inflamed tissues, which are likely to be acidified [4,5].

Given the transient nature of severe inflammation, it seemed likely that the timing of pHLIP delivery would impact the extent of pHLIP targeting. We therefore asked whether pHLIP targets lung tissue at earlier times postinfection by injecting pHLIP at days 1 and 5 postinfection (Supplementary Figure 1A) (see online www.futuremedicine.com/doi/suppl/10.2217/FMB.12.134). Results show that pHLIP did not target the lungs of infected mice when administered 1 day postinfection, and could be found in only one out of three mice if

given 5 days postinfection (Supplementary Figure 1B). Our group previously reported PR8 infection of bronchiolar and alveolar epithelial cells during the early stages of infection and the disappearance of influenza antigens by day 9 postinfection [15]. Interestingly, immune cell infiltration was reduced in the lung parenchyma when viral infection was apparent. The lack of pHLIP in tissue during the window of virus replication suggests that the infection alone does not facilitate entry of pHLIP into the lung tissue. Cellular inflammation may therefore be important in generating a microenvironment that enables pHLIP targeting of damaged lung tissue.

Subcellular location of pHLIP

Previous studies have shown that pHLIP inserts into membranes in a pH-dependent fashion [17,18]. Here, we tested the ability of pHLIP to specifically bind to human lung adenocarcinoma cells. As shown in Figure 4A, pHLIP indeed binds to the surface of A549 cells in a pH-dependent fashion. Consistent with these observations, pHLIP also bound to Raji cells (a B-cell lymphoma line) at low pH (data not shown). To explore the possibility that pHLIP is extra cellular *in vivo*, we visualized fibronectin, a protein that is present in inflamed lung tissue within the extracellular matrix. Interestingly, some pHLIP can also be found in the same regions of polymer ized fibronectin (Figure 4B). This result shows that pHLIP is indeed extracellular, and suggests that pHLIP may be on the surface of cells and also within the extracellular matrix, possibly as a result of entrapment.

To more specifically visualize cell membranes, we stained infected lungs for membrane glycoproteins using WGA, which is pseudocolored green in Figure 4C. In the heavily infiltrated regions, some pHLIP is found sandwiched in between WGA, colocalized with WGA or at the boundaries of DAPI stains, suggesting close proximity to the cell membranes. Although it is difficult to discern specific binding of pHLIP at the cell membranes, fluorophores conjugated to pHLIP that are singly inserted into cell membranes are not likely to be easily detected by epifluorescent or confocal microscopy. Given that pHLIP inserts into cell membranes at low pH, it is likely that pHLIP is also inserted into cell membranes at the sites of infiltration.

pHLIP colocalizes with damaged lung tissue

The alveolar spaces within the lungs are populated with pneumocytes that are required for gaseous exchange. We investigated the association of pHLIP with two pneumocytes: ATI and ATII. Each cell type can be visualized via secondary staining of antibodies for cell type-specific markers: Pdpn for ATI cells and the C-terminus of SPC for ATII cells. Figure 5A shows that, in influenza-infected lungs, ATI and ATII are prominently present throughout the alveolar parenchyma (stained yellow and green, respectively) in healthy portions of the lung. By contrast, pHLIP is clearly concentrated in regions of severe infiltration that are largely devoid of Pdpn-positive ATI and SPC-positive ATII cells (darker regions).

Narasaraju *et al.* described that the loss of continuity in Pdpn (also known as T1-α) immunostaining in mouse lung parenchyma is an indication of type I pneumocyte damage [19]. Using a program that we designed to enable quantification of staining intensity and extent of overlay (see ‘Materials & methods’ section), the percentage of pHLIP-derived pixels in Pdpn-positive and Pdpn-negative areas was quantified. While 84% of pHLIP coincides with Pdpn-negative areas, only 16% of pHLIP is found in Pdpn-positive areas (Figure 5B). Figure 5C demonstrates the method of quantification. It shows that uninfected lung (top panel) is entirely stained Pdpn positive (column 3) and that pHLIP is not detected in the uninfected lung (column 2). In infected mouse lungs (bottom panel), pHLIP (column 2) does not greatly overlap with the Pdpn-positive regions (column 3); the extent of overlap is shown in column 4. However, a substantial amount of pHLIP coincides with Pdpn-

negative areas (column 5). The extent of overlap is shown in column 6 of Figure 5. Severe pulmonary inflammation has been attributed to be a cause of pneumocyte death under several conditions [20–23]. Therefore, pHLIP predominantly targets lung parenchyma where there is damage to epithelial pneumocytes and where pulmonary function is compromised.

pHLIP targets lung parenchyma with diminished Prdx6 expression

Besides gaseous exchange, pneumocytes produce several critical antioxidants to protect themselves against oxidative stress, including Prdx6, a bifunctional GSH peroxidase that reduces hydrogen peroxides and lipid hydroperoxides by utilizing GSH [24]. In previous studies, we showed that there is a transient induction of Prdx6 in ATI cells in response to infiltration, but complete disappearance of Prdx6 in consolidated alveoli, possibly due to depletion of ATI cells [15]. We therefore investigated Prdx6 distribution in these studies by using fluorescent antibodies to assess the distribution of Prdx6 relative to the location of pHLIP. Prdx6 has been shown to confer significant protection against oxidative stress-induced lung injuries [25,26]. Consistent with this previous report, while Prdx6 is predominantly expressed in bronchiolar epithelial cells of un infected mice (Figure 6A i, iv, vii & x), its expression is induced in the alveolar epithelium of moderately infiltrated lungs where only sparsely distributed pHLIP can be found at regions neighboring heavily infiltrated sites (Figure 6A ii, v, viii & xi). However, Prdx6 expression is severely diminished in the alveoli of heavily infiltrated/inflamed lungs (Figure 6A iii, ix & xii). Remarkably, when pHLIP is injected into infected mice, it specifically targets regions of the lung that are deficient in Prdx6 (i.e., heavily infiltrated regions) (Figure 6A iii, vi, ix & xii). Indeed, approximately 90% of pHLIP-induced fluorescence resides in Prdx6-negative regions, whereas only approximately 10% of the remaining pHLIP-induced fluorescence can be found in Prdx6-positive regions (Figure 6B). The method of quantification is briefly demonstrated in Figure 6C, where the total Prdx6-positive area (column 2) is identified based on anti-Prdx6 staining (column 1). The percentage of pHLIP that overlaps with Prdx6-positive areas (column 3) and Prdx6-negative areas (column 4) were then computed. These data show that pHLIP is abundant precisely where Prdx6 is deficient, suggesting opportunities for therapeutic targeting using conjugates of pHLIP with agents that principally compensate for loss of antioxidant protection in inflamed regions of the lung.

A pH-insensitive pHLIP variant targets damaged lung tissue of influenza-infected mice

Previous studies have shown that by changing two aspartates to lysines within the pHLIP sequence, the pH-dependent protonation is eliminated, rendering the peptide incapable of secondary conformation change and pH-dependent insertion into the lipid bilayer [3]. This variant sequence, termed K-pHLIP, was labeled with Hylite Fluor 647 and injected into influenza-infected mice, analogously to the pHLIP peptide. K-pHLIP cannot be protonated and thus is unresponsive to acidic pH. Indeed, unlike pHLIP, K-pHLIP does not have any significant affinity for the acidic kidney cortex (Supplementary Figure 2A). Interestingly, we observed that K-pHLIP retained at least some of its ability to target inflamed regions of the lung (Supplementary Figure 2B). These data suggest the possibility that pHLIP may target damaged lung tissue due to a pH-dependent conformational change and/or via another mechanism that is pH independent. Additional mechanisms of action may add to the robustness of pHLIP as an agent for targeting damaged lung tissue during influenza.

Discussion

Influenza-induced pneumonia is a rare but serious pulmonary manifestation of the viral infection that is recognizable by multifocal radiographic consolidation indicating signs of cell infiltration [27]. Statistics show that patients suffering from pneumonia during the 2009 H1N1 pandemic were more likely to be admitted to intensive care units, suffer from acute

respiratory distress syndromes, experience sepsis and suffer morbidity [12]. Since a general consequence of infection and inflammation is acidification of tissue, the application of the pHLIP peptide may enable specific targeting of imaging and therapeutic agents to inflamed foci of the lungs during severe influenza infections. Our objective of this study was to explore the potential utility of pHLIP in applications related to infectious diseases. Here, we report the distribution of pHLIP in influenza-infected mice, thus revealing its potential usage as a bioimaging tool or drug-delivery agent for severe influenza infections.

Our data demonstrate that pHLIP specifically directed fluorophores to damaged lung parenchyma, characterized by heavy immune cell infiltration. pHLIP-targeted regions are also characterized by compromised alveoli architecture and severe depletion of a key lung antioxidant, Prdx6. The ability of pHLIP to specifically target inflamed and damaged lung tissue creates an opportunity for the delivery of pharmaceutical compounds aimed at ameliorating lung injury at the affected tissue.

A careful examination of multiple tissues showed that, consistent with previous studies, pHLIP also targets the kidneys (data not shown). Relatively little pHLIP was observed in other tissues, as has been previously described. Development of pHLIP conjugates will therefore need to take into consideration possible side effects in the kidneys, although sodium bicarbonate can be added to the diet to increase the pH of the organs, thus reducing nonspecific delivery [3].

A key finding of this study is that pHLIP specifically targets heavily infiltrated regions of influenza-infected mouse lungs. In addition, while pHLIP is appreciably detectable in the lungs during later stage of infection, it does not target infected lungs as effectively during earlier time points. This suggests that cellular or molecular events that take place during the later stages of PR8 infection create a microenvironment that is conducive for pHLIP targeting.

Local acidosis has been found to arise from the production of lactic acid by metabolically active polymorphonuclear cells [28]; pHLIP targeting at the later stages of infection may be a result of lactic acid accumulation due to highly active, densely packed immune cells. Additionally, during the later stages of infection predominated by activation of the adaptive host responses, activated and proliferating T lymphocytes undergo aerobic glycolysis to meet the demand of their rapid energy consumption, thus creating a microenvironment with increased lactate [29]. This evidence is consistent with the specific targeting of pHLIP to inflamed regions of the lungs.

It is also possible that in addition to pH-dependent insertion, there are additional mechanisms for pHLIP localization in infected mouse lungs. The observation that the K-pHLIP variant can target sites of inflammation during influenza suggests that these peptides share an attribute that allows for targeting in a pH-independent fashion. Studies of mice implanted with tumors show that, unlike pHLIP, K-pHLIP does not target acidic tumors and has appreciably less distribution in the kidneys, liver, blood and spleen. However, similar distribution was observed in the lung, possibly because the lung is a highly vascularized organ that has better retention of K-pHLIP [30]. Additionally, K-pHLIP is thought to have a partial α-helical structure, even at normal pH [3], and it may also form aggregates with the ability to penetrate the leaky vasculature associated with inflammation. K-pHLIP might therefore become trapped in the complex milieu of the inflamed lung matrix, in a phenomenon known as the enhanced permeability and retention effect. Regardless of the mechanisms that underlie its activities, it is clear that pHLIP is highly effective in targeted sites of influenza-induced inflammation.

Potential clinical application

The selection of therapeutic agents based on the biodistribution profile of pHLIP is critical in the success of pHLIP-based drug-delivery systems. Localization of pHLIP specifically at regions where healthy pneumocytes are already depleted suggests that it may be too late for treatments that prevent inflammation-induced injury to lung epithelial cells. However, at this stage, the recovery of lung epithelial cells is highly critical to the survival of influenza patients. In fact, there is a growing interest in stem cell therapies or growth factors that can be exploited to facilitate regeneration of damaged lungs [16,31,32]. Ultimately, both traditional and novel therapeutics might be more effective when delivered with pHLIP-potentiated targeting.

The observation of pHLIP targeting Prdx6-depleted regions raises the possibility of using pHLIP to deliver agents that specifically compensate for the redox imbalance caused by Prdx6 depletion. Prdx6 has been reported to be the most critical enzyme for reducing oxidized phospholipids in the lungs [33]. Not only are oxidized phospholipids highly reactive and capable of propagating reactive oxygen species, they have also been shown to mediate acute lung injury [34] and may be involved in inducing T cells to break tolerance towards self-protein [35]. Hence, a possible future direction is to develop pHLIP–Prdx6 conjugates to protect and restore lung tissue during influenza.

When considering factors that might impact the efficacy of pHLIP–Prdx6 conjugates, the impact of pH on Prdx6 needs to be taken into consideration. The GSH peroxidase (antioxidant) activity of Prdx6 functions maximally at physiological pH and is reduced at low pH. On the other hand, phospholipase A_2 activity is maximal in pH 4 microenvironments, which can be found in highly acidic intracellular compartments, such as lysosomes and endosomes [36]. Given that extremely low pH is unlikely to be present in the interstitium of lung tissue, one potential strategy to deliver antioxidant activity of Prdx6 but exclude phospholipase A_2 activity is to mutate a catalytic triad, which is necessary for phospholipase A_2 activities [37]. Furthermore, in addition to Prdx6, there are numerous additional candidate antioxidants that can be delivered to sites of Prdx6 deficiency in order to reduce oxidative stress in influenza patients. pHLIP provides a potential vehicle for achieving this aim.

Drawing from observations of H1N1 pandemic and H5N1 avian influenza patients, a significant portion of critically ill patients with viral pneumonia never recover despite intensive care. Autopsies show that diffuse alveolar damage, intra-alveolar edema and cellular infiltration are some of the major histopathological findings [2,38–42], which are consistent with the findings in this study. Excessive infiltration of immune cells and injury to the lung parenchyma can compromise gaseous exchange by reducing lung volume and compliance [43]. The observation that pHLIP preferentially targets infiltrated sites suggests that conjugates that combine pHLIP with anti-inflammatory agents could be exploited to suppress oxidative stress at sites of infiltration. Importantly, targeted delivery would also reduce exposure of normal healthy portions of the lung to therapeutic agents. Given that anti-inflammatory agents can be deleterious in healthy portions of the lung, where they suppress antiviral responses and cause side effects, targeting is thus advantageous both because it can increase the local concentration of therapeutic agents at sites where they are needed, while at the same time preventing disruption of normal pulmonary physiology in healthy portions of the lung.

Conclusion

This study delineates the distribution of a pH-sensitive peptide, pHLIP, in a severe influenza infection model, and sets the foundation for selecting candidate agents that can be

conjugated to pHLIP for therapeutic purposes. Future pandemics are inevitable. While the development of new vaccines and antivirals is key, it is also important to develop alternative approaches, such as targeted drug delivery, which shows promise as a means to offset morbidity and mortality rates.

Supplementary Material

Refer to Web version on PubMed Central for supplementary material.

Acknowledgments

The authors would like to thank MC Phoon for propagating the virus and JE Seet for her expert opinions on lung histology.

This publication is made possible by the Singapore National Research Foundation and is administered by the Singapore–MIT Alliance for Research and Technology. This work was also supported in part by the National Institute of Environmental Health Sciences (P01-ES006052). DM Engelward is supported by NIH grant GM073857. More than one party is a coauthor on a patent for pHLIP development. Currently, pHLIP has not yet been formally licensed.

No writing assistance was utilized in the production of this manuscript.

References

Papers of special note have been highlighted as:

■ of interest

■■ of considerable interest

1. La Gruta NL, Kedzierska K, Stambas J, Doherty PC. A question of self-preservation: immunopathology in influenza virus infection. Immunol. Cell Biol. 2007; 85(2):85–92. [PubMed: 17213831]
2. Howard WA, Peiris M, Hayden FG. Report of the ‘Mechanisms of Lung Injury and Immunomodulator Interventions in Influenza’ workshop, 21 March 2010, Ventura, California, USA. Influenza Other Respi. Viruses. 2011; 5(6):453–454. e458–e475. [PubMed: 21848616]
3. Andreev OA, Dupuy AD, Segala M, et al. Mechanism and uses of a membrane peptide that targets tumors and other acidic tissues *in vivo*. Proc. Natl Acad. Sci. USA. 2007; 104(19):7893–7898. [PubMed: 17483464] ■■ pH (low) insertion peptide targets acidic tissues such as tumors and arthritic joints.
4. Segala J, Engelman DM, Reshetnyak YK, Andreev OA. Accurate analysis of tumor margins using a fluorescent pH low insertion peptide (pHLIP). Int. J. Mol. Sci. 2009; 10(8):3478–3487. [PubMed: 20111691]
5. Andreev OA, Engelman DM, Reshetnyak YK. Targeting acidic diseased tissue: new technology based on use of the pH (low) insertion peptide (pHLIP). Chim. Oggi. 2009; 27(2):34–37. [PubMed: 20037661]
6. Reshetnyak YK, Yao L, Zheng S, Kuznetsov S, Engelman DM, Andreev OA. Measuring tumor aggressiveness and targeting metastatic lesions with fluorescent pHLIP. Mol. Imaging Biol. 2011; 13(6):1146–1156. [PubMed: 21181501]
7. Reshetnyak YK, Andreev OA, Lehnert U, Engelman DM. Translocation of molecules into cells by pH-dependent insertion of a transmembrane helix. Proc. Natl Acad. Sci. USA. 2006; 103(17):6460–6465. [PubMed: 16608910] ■ The biophysical properties of pH (low) insertion peptide enable it to either tether molecules on the extracellular surface of the plasma membrane or translocate molecules across the cell membrane into the cytosol.
8. An M, Wijesinghe D, Andreev OA, Reshetnyak YK, Engelman DM. pH-(low)-insertion-peptide (pHLIP) translocation of membrane impermeable phalloidin toxin inhibits cancer cell proliferation. Proc. Natl Acad. Sci. USA. 2010; 107(47):20246–20250. [PubMed: 21048084]

9. Thevenin D, An M, Engelman DM. pHLIP-mediated translocation of membrane-impermeable molecules into cells. Chem. Biol. 2009; 16(7):754–762. [PubMed: 19635412]
10. Punnia-Moorthy A. Evaluation of pH changes in inflammation of the subcutaneous air pouch lining in the rat, induced by carrageenan, dextran and *Staphylococcus aureus*. J. Oral Pathol. 1987; 16(1):36–44. [PubMed: 2435877]
11. Martin GR, Jain RK. Fluorescence ratio imaging measurement of pH gradients: calibration and application in normal and tumor tissues. Microvasc. Res. 1993; 46(2):216–230. [PubMed: 8246820]
12. Jain S, Benoit SR, Skarbinski J, Bramley AM, Finelli L. Influenza-associated pneumonia among hospitalized patients with 2009 pandemic influenza A (H1N1) virus – United States, 2009. Clin. Infect. Dis. 2012; 54(9):1221–1229. [PubMed: 22437239]
13. Buchweitz JP, Harkema JR, Kaminski NE. Time-dependent airway epithelial and inflammatory cell responses induced by influenza virus A/PR/8/34 in C57BL/6 mice. Toxicol. Pathol. 2007; 35(3):424–435. [PubMed: 17487773]
14. Srivastava B, Blazejewska P, Hessmann M, et al. Host genetic background strongly influences the response to influenza A virus infections. PLoS One. 2009; 4(3):e4857. [PubMed: 19293935]
15. Yamada Y, Limmon GV, Zheng D, et al. Major shifts in the spatio–temporal distribution of lung antioxidant enzymes during influenza pneumonia. PLoS One. 2012; 7(2):e31494. [PubMed: 22355371]
16. Kumar PA, Hu Y, Yamamoto Y, et al. Distal airway stem cells yield alveoli *in vitro* and during lung regeneration following H1N1 influenza infection. Cell. 2011; 147(3):525–538. [PubMed: 22036562]
17. Andreev OA, Karabadzhak AG, Weerakkody D, Andreev GO, Engelman DM, Reshetnyak YK. pH (low) insertion peptide (pHLIP) inserts across a lipid bilayer as a helix and exits by a different path. Proc. Natl Acad. Sci. USA. 2010; 107(9):4081–4086. [PubMed: 20160113]
18. Reshetnyak YK, Andreev OA, Segala M, Markin VS, Engelman DM. Energetics of peptide (pHLIP) binding to and folding across a lipid bilayer membrane. Proc. Natl Acad. Sci. USA. 2008; 105(40):15340–15345. [PubMed: 18829441]
19. Narasaraju T, Ng HH, Phoon MC, Chow VT. MCP-1 antibody treatment enhances damage and impedes repair of the alveolar epithelium in influenza pneumonitis. Am. J. Respir. Cell Mol. Biol. 2010; 42(6):732–743. [PubMed: 19617401]
20. Perl M, Lomas-Neira J, Chung CS, Ayala A. Epithelial cell apoptosis and neutrophil recruitment in acute lung injury – a unifying hypothesis? What we have learned from small interfering RNAs. Mol. Med. 2008; 14(7–8):465–475. [PubMed: 18368145]
21. Smani Y, Docobo-Perez F, McConnell MJ, Pachon J. *Acinetobacter baumannii*-induced lung cell death: role of inflammation, oxidative stress and cytosolic calcium. Microb. Pathog. 2011; 50(5): 224–232. [PubMed: 21288481]
22. Rock KL. Pathobiology of inflammation to cell death. Biol. Blood Marrow Transplant. 2009; 15(1 Suppl.):137–138. [PubMed: 19147093]
23. Bergeron Y, Ouellet N, Deslauriers AM, Simard M, Olivier M, Bergeron MG. Cytokine kinetics and other host factors in response to pneumococcal pulmonary infection in mice. Infect. Immun. 1998; 66(3):912–922. [PubMed: 9488375]
24. Fisher AB. Peroxiredoxin 6: a bifunctional enzyme with glutathione peroxidase and phospholipase A activities. Antioxid. Redox Signal. 2011; 15(3):831–844. [PubMed: 20919932]
25. Wang Y, Phelan SA, Manevich Y, Feinstein SI, Fisher AB. Transgenic mice overexpressing peroxiredoxin 6 show increased resistance to lung injury in hyperoxia. Am. J. Respir. Cell Mol. Biol. 2006; 34(4):481–486. [PubMed: 16399955]
26. Yang D, Song Y, Wang X, et al. Deletion of peroxiredoxin 6 potentiates lipopolysaccharide-induced acute lung injury in mice. Crit. Care Med. 2011; 39(4):756–764. [PubMed: 21200322]
27. Nicolini A, Ferrera L, Rao F, Senarega R, Ferrari-Bravo M. Chest radiological findings of influenza A H1N1 pneumonia. Rev. Port. Pneumol. 2012; 18(3):120–127. [PubMed: 22483844]
28. Menkin V. Biochemical mechanisms in inflammation. BMJ. 1960; 1(5185):1521–1528. [PubMed: 20788900]

29. Frauwirth KA, Thompson CB. Regulation of T lymphocyte metabolism. J. Immunol. 2004; 172(8): 4661–4665. [PubMed: 15067038]
30. Daumar P, Wanger-Baumann CA, Pillarsetty N, et al. Efficient ^{18}F-labeling of large 37-amino-acid pHLIP peptide analogues and their biological evaluation. Bioconjug. Chem. 2012; 23(8): 1557–1566. [PubMed: 22784215]
31. Yanagita K, Matsumoto K, Sekiguchi K, Ishibashi H, Niho Y, Nakamura T. Hepatocyte growth factor may act as a pulmotrophic factor on lung regeneration after acute lung injury. J. Biol. Chem. 1993; 268(28):21212–21217. [PubMed: 8407957]
32. Rennard SI, Wachenfeldt K. Rationale and emerging approaches for targeting lung repair and regeneration in the treatment of chronic obstructive pulmonary disease. Proc. Am. Thorac. Soc. 2011; 8(4):368–375. [PubMed: 21816994]
33. Liu G, Feinstein SI, Wang Y, et al. Comparison of glutathione peroxidase 1 and peroxiredoxin 6 in protection against oxidative stress in the mouse lung. Free Radic. Biol. Med. 2010; 49(7):1172–1181. [PubMed: 20627125]
34. Imai Y, Kuba K, Neely GG, et al. Identification of oxidative stress and Toll-like receptor 4 signaling as a key pathway of acute lung injury. Cell. 2008; 133(2):235–249. [PubMed: 18423196]
35. Wuttge DM, Bruzelius M, Stemme S. T-cell recognition of lipid peroxidation products breaks tolerance to self proteins. Immunology. 1999; 98(2):273–279. [PubMed: 10540227]
36. Wu YZ, Manevich Y, Baldwin JL, et al. Interaction of surfactant protein A with peroxiredoxin 6 regulates phospholipase A2 activity. J. Biol. Chem. 2006; 281(11):7515–7525. [PubMed: 16330552]
37. Manevich Y, Shuvaeva T, Dodia C, Kazi A, Feinstein SI, Fisher AB. Binding of peroxiredoxin 6 to substrate determines differential phospholipid hydroperoxide peroxidase and phospholipase A_2 activities. Arch. Biochem. Biophys. 2009; 485(2):139–149. [PubMed: 19236840]
38. Valente T, Lassandro F, Marino M, Squillante F, Aliperta M, Muto R. H1N1 pneumonia: our experience in 50 patients with a severe clinical course of novel swine-origin influenza A (H1N1) virus (S-OIV). Radiol. Med. 2012; 117(2):165–184. [PubMed: 22020427]
39. Soepandi PZ, Burhan E, Mangunnegoro H, et al. Clinical course of avian influenza A(H5N1) in patients at the Persahabatan Hospital, Jakarta, Indonesia, 2005–2008. Chest. 2010; 138(3):665–673. [PubMed: 20507944]
40. Bay A, Etlik O, Oner AF, et al. Radiological and clinical course of pneumonia in patients with avian influenza H5N1. Eur. J. Radiol. 2007; 61(2):245–250. [PubMed: 17110072]
41. Nakajima N, Sato Y, Katano H, et al. Histopathological and immunohistochemical findings of 20 autopsy cases with 2009 H1N1 virus infection. Mod. Pathol. 2012; 25(1):1–13. [PubMed: 21874012]
42. Korteweg C, Gu J. Pathology, molecular biology, and pathogenesis of avian influenza A (H5N1) infection in humans. Am. J. Pathol. 2008; 172(5):1155–1170. [PubMed: 18403604]
43. Korotzer TI, Weiss HS, Hamparian VV, Somerson NL. Oxygen uptake and lung function in mice infected with *Streptococcus pneumoniae*, influenza virus, or *Mycoplasma pulmonis*. J. Lab. Clin. Med. 1978; 91(2):280–294. [PubMed: 23401]

Executive summary

- Fluorescently labeled pH (low) insertion peptide (pHLIP) targets influenza-infected mouse lungs at sites of dense cellular infiltration present during the later stages of infection (85% of pHLIP colocalizes to sites of dense infiltration).
- pHLIP is detectable in close proximity to glycoproteins found on cell membranes, which suggests that pHLIP is associated with the plasma membrane.
- Approxmately 84% of fluorescently labeled pHLIP colocalizes with tissues devoid of podoplanin-expressing alveolar type I (ATI) cells, whereas only approximately 16% of pHLIP is located in healthy lung tissues with podoplanin-expressing ATI cells.
- Lung tissue targeted by pHLIP has diminished Prdx6 levels, which is consistent with the depletion of ATI cells that normally express Prdx6.
- A pHLIP variant, known as K-pHLIP, which is mutated by two amino acids to render it insensitive to low pH, also localizes to inflamed lung tissue, suggesting the possibility that more than one mechanism underlies the efficacy of pHLIP targeting.
- The ability of pHLIP to effectively target inflamed regions of the lung that are deficient in antioxidants opens new therapeutic angles, including targeted delivery of antioxidants and agents that promote tissue regeneration.

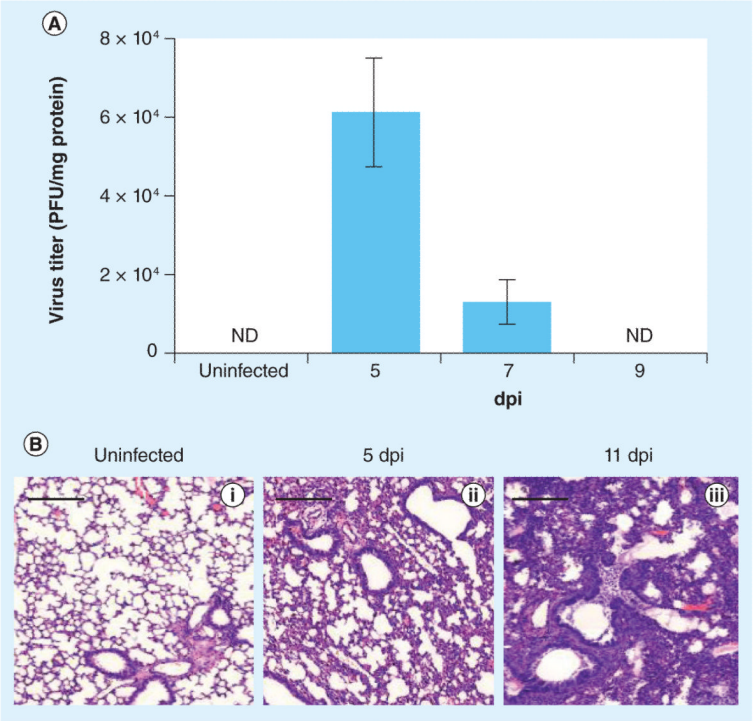

Figure 1. Infection kinetics of Influenza A in mouse lungs

(A) Quantification of viral plaques from lung homogenates. PFUs are normalized to milligrams of protein in the lung homogenates (measured by Bradford assay) and represented as PFU ± standard deviation. **(B)** Prolonged inflammation in the lungs of influenza A/Puerto Rico/8/34-infected mice. Representative hematoxylin and eosin diagrams show **(i)** normal alveolar structure in uninfected mouse lung, **(ii)** thickening of alveolar walls with infiltration of immune cells on 5 dpi and **(iii)** severe lung infiltration and disrupted alveolar structures on 11 dpi, after virus has been cleared (n = 3).

Scale bars: 200 μm.

dpi: Days postinfection; ND: Not determined.

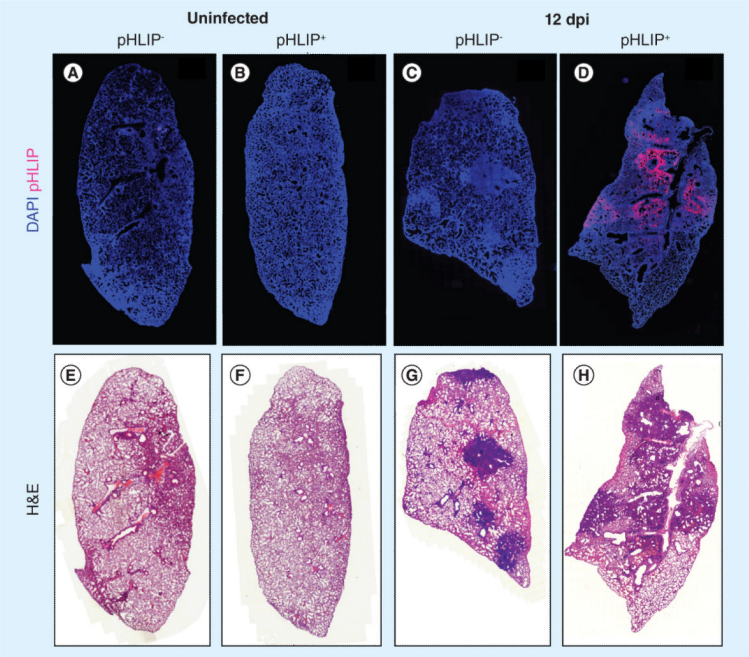

Figure 2. pH (low) insertion peptide targets infected but not uninfected mouse lungs

Representative whole-lung images from three independent experiments (n ≥4). pHLIP was administered to influenza A/Puerto Rico/8/34-infected mice on day 10 postinfection. **(A–D)** DAPI (blue) and pHLIP (red). **(B & D)** At 12 dpi, pHLIP can only be detected in infected lungs.

(A & C) Control lungs from uninfected and infected mice. **(E–H)** H&E staining of the same samples. Darkened areas indicate regions of immune cell infiltration and inflammation.

dpi: Days postinfection; H&E: Hematoxylin and eosin; pHLIP: pH (low) insertion peptide.

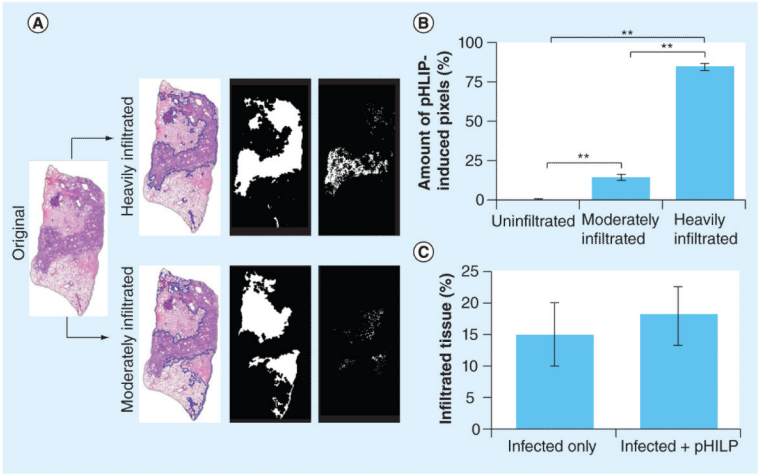

Figure 3. pH (low) insertion peptide targets heavily infiltrated lung tissue

(A) Method of quantification for pHLIP in different regions of the lungs. Original hematoxylin and eosin images (left-most column) were segmented to distinguish heavily infiltrated and moderately infiltrated regions, which are traced in blue lines in the second column. Alveoli, bronchi and blood vessels were filled to generate alveolar areas, as shown in the third column. The total amount of pHLIP-induced fluorescence that overlapped with these alveolar areas (as shown in the right-most column) was then quantified. **(B)** pHLIP preferentially targets heavily infiltrated regions. Only 1.4 ± 0.7% of total pHLIP was found in uninfiltrated regions, while 13.7 ± 2.9% of pHLIP was found in moderately infiltrated regions and 84.9 ± 2.7% of pHLIP was found in heavily infiltrated regions. The percentage of pHLIP in different regions was calculated using two lung sections per mouse (n = 3). Bars indicate standard error of the mean. **(C)** pHLIP injection does not affect the degree of infiltration into mice lungs. Ten 5-μm thick lung sections at least 50 μm apart were obtained from infected mice injected or not injected with Hylite Fluor® 647 pHLIP. They were stained with hematoxylin and eosin and the percentage of heavily infiltrated tissue was quantified (n = 5). Data show that there is no significant difference between percentages of infiltration between these two groups.

**$p < 0.01$ (Student's *t*-test).

pHLIP: pH (low) insertion peptide.

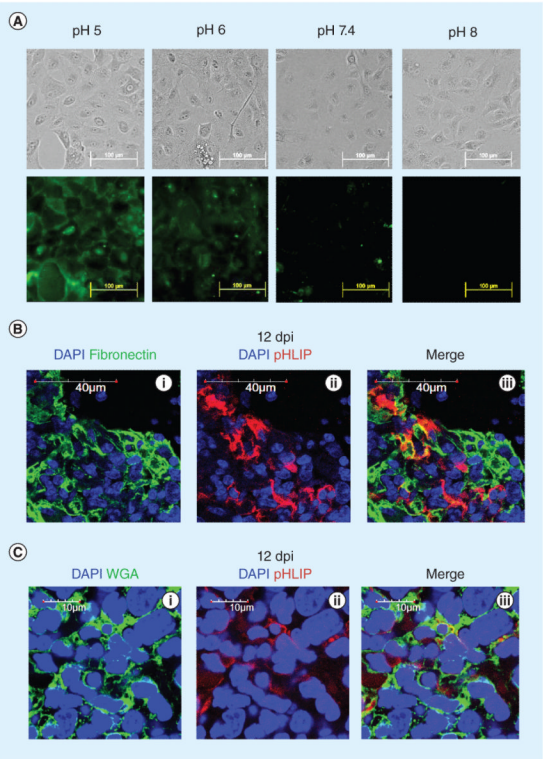

Figure 4. pH (low) insertion peptide targets cellular membrane and extracellular matrix

(A) pHLIP preferentially binds to the cell membrane at acidic pH *in vitro*. A549 cells were incubated with 8 μM of 5-carboxyfluorescein-conjugated pHLIP under different pH conditions. 5-carboxyfluorescein-conjugated pHLIP binds to the cell membrane of A549 cells at acidic pH of 5 and 6, but not at alkaline pH of 7.4 and 8. **(B)** Fibrillar fibronectin (green) delineates the extracellular space where some pHLIP (red) can be found (60× magnification). **(C)** pHLIP is in close proximity to WGA-stained cell membrane glycoprotein (100× magnification). WGA stains the cell membrane (green) of influenza-infected mouse lungs. In the heavily infiltrated regions, thin streaks of pHLIP (red) run around the perimeter of cells and are sandwiched by or colocalize with WGA staining, suggesting close proximity to the cell membrane.

dpi: Days postinfection; pHLIP: pH (low) insertion peptide; WGA: Wheat germ agglutinin.

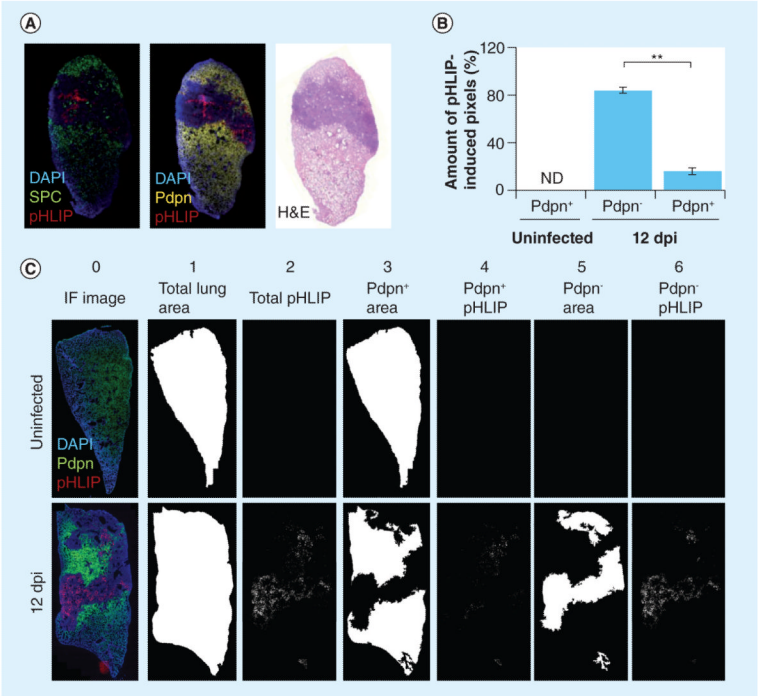

Figure 5. pH (low) insertion peptide targets damaged lung tissue

(A) pHLIP targets damaged lung tissue devoid of normal alveolar type I (ATI) and alveolar type II (ATII) cells. Representative images of lungs sections stained with anti-SPC and anti-Pdpn. pHLIP (red) does not colocalize with SPC^+ ATII (green) or $Pdpn^+$ ATI cells (yellow). **(B)** pHLIP is mostly observed in regions devoid of $Pdpn^+$ ATI cells. The percentages of $pHLIP^+$ pixels in $Pdpn^+$ and $Pdpn^-$ regions were calculated using two lung sections per mouse (n = 3). There are significantly more pHLIP-induced pixels in $Pdpn^-$ regions (84.1 ± 2.7%) compared with $Pdpn^+$ regions (15.9 ± 2.7%) of influenza A/Puerto Rico/8/34-infected mice. Bars indicate standard error of the mean. **(C)** Coincidence of $pHLIP^+$ regions and $Pdpn^+$ and $Pdpn^-$ regions. Total area of lung sections (column 1) according to DAPI staining (column 0). $Pdpn^+$ areas (column 3) and $Pdpn^-$ areas (column 5) were imaged and quantified according to Pdpn immunohistochemistry. Total pHLIP staining is shown in column 2 and pHLIP staining that coincides with $Pdpn^+$ or $Pdpn^-$ regions are shown in columns 4 and 6, respectively.

**$p < 0.01$ (Student's *t*-test).

dpi: Days postinfection; H&E: Hematoxylin and eosin; IF: Immunofluorescence; ND: Not determined; Pdpn: Podoplanin; pHLIP: pH (low) insertion peptide; SPC: Surfactant protein C.

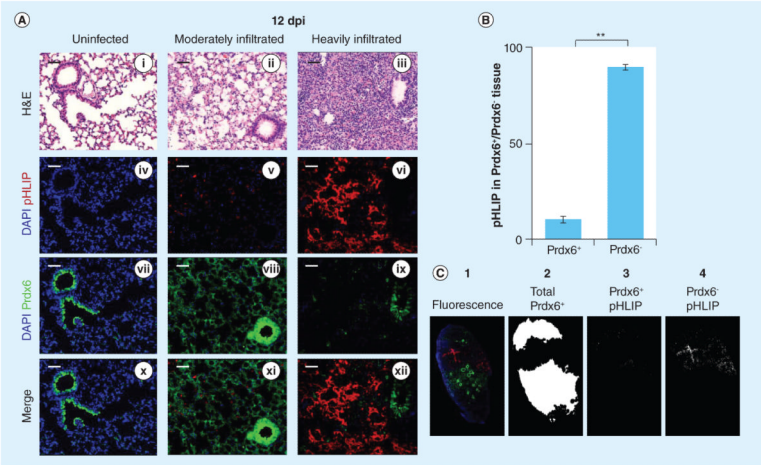

Figure 6. pH (low) insertion peptide targets regions devoid of Prdx6

(A) pHLIP localizes at lung tissue depleted of Prdx6. **(i, vii & x)** Prdx6 (green) is expressed at baseline level in the alveolar epithelium of uninfected mouse lungs. **(iv)** No pHLIP was found in the uninfected lung tissue. **(ii, viii & xi)** Prdx6 is elevated in moderately infiltrated tissue of infected mouse lungs, where **(v, xi)** sparsely distributed pHLIP can only be found at sites immediately neighboring heavily infiltrated tissue. **(iii, vi, ix & xii)** pHLIP mainly targets inflamed sites with diminished Prdx6 expression both in the alveolar and the bronchiolar epithelial cells. **(B)** The percentages of pHLIP fluorescence in $Prdx6^+$ and $Prdx6^-$ regions were calculated with two immunofluorescently labeled lung sections per mouse (n = 3). pHLIP-induced pixels are almost exclusively found in $Prdx6^-$ regions (89.7 ± 3.3%). Significantly less pHLIP can be detected in $Prdx6^+$ regions (10.3 ± 3.3%) of influenza A/Puerto Rico/8/34-infected mice. Bars are shown as mean ± standard error of the mean. **(C)** Coincidence of pHLIP fluorescence with regions of Prdx6 immunofluorescence was identified. Fluorescence image of whole-lung sections stained with anti-Prdx6 (column 1) was quantified by separating Prdx6 (green) and pHLIP (red) channels. $Prdx6^+$ regions were identified (column 2) and percentages of pHLIP residing in $Prdx6^+$ (column 3) and $Prdx6^-$ (column 4) regions were quantified.

**$p < 0.01$ for percentage of pHLIP-induced fluorescence in $Prdx6^+$ lung tissue compared with $Prdx6^-$ lung tissue in influenza A/Puerto Rico/8/34-infected mice.

Scale bars: 100 μm.

dpi: Days postinfection; H&E: Hematoxylin and eosin; pHLIP: pH (low) insertion peptide.